arXiv:0804.3805v3 [hep-ph] 10 Nov 2008

A systematic study of direct photon production in heavy ion collisions

Ivan Vitev[1] and Ben-Wei Zhang[1,2]
[1] *Los Alamos National Laboratory, Theoretical Division,*
Mail Stop B283, Los Alamos, NM 87545, USA and
[2] *Institute of Particle Physics, Hua-Zhong Normal University, Wuhan 430079, China*

(Dated: November 10, 2008)

A theoretical derivation of photon bremsstrahlung, induced by the interactions of an energetic quark in a hot and dense quark-gluon plasma, is given in the framework of the reaction operator approach. For the physically relevant case of hard jet production, followed by few in-medium interactions, we find that the Landau-Pomeranchuk-Migdal suppression of the bremsstrahlung photon intensity is much stronger than in the previously discussed limit of on-shell quarks and a large number of soft scatterings. This result is incorporated in the first systematic study of direct photon production in minimum bias d+Cu and d+Au and central Cu+Cu and Au+Au heavy ion collisions at the Relativistic Heavy Ion Collider at center of mass energies $\sqrt{s} = 62.4$ GeV and 200 GeV. We find that the contribution of the photons created via final-state interactions is limited to 35% for 2 GeV$< p_T < 5$ GeV and at high transverse momenta the modification of the direct photon cross section is dominated by initial-state cold nuclear matter effects.

PACS numbers: 12.38.Bx,12.38.Mh,24.85.+p,25.75.-q,25.75.Cj

I. INTRODUCTION

In the highly successful hard probes program at the Relativistic Heavy Ion Collider (RHIC), the interplay of nuclear effects that alter the cross section for direct photon production is not yet well understood. Direct γ measurements [1, 2] have provided an important baseline to help establish the dominance of final-state effects for the observed large suppression of energetic hadrons [3, 4, 5] in nucleus-nucleus collisions. The interest of the theoretical community, however, has been centered on possibly large new sources of photons as a by-product of an energetic parton propagating in the quark-gluon plasma (QGP) [6]. Early work predicted significant enhancement of low to intermediate p_T photons [7, 8] based on a γ emission pattern characteristic of on-shell quarks and a very large number of soft interactions in matter, e.g. [9]. This limit yields only a small, $\sim 30\%$, Landau-Pomeranchuk-Migdal (LPM) suppression of the photon spectrum relative to the incoherent Bethe-Heitler result. It does not reflect, however, the possibly large cancellation between the bremsstrahlung associated with hard jet production and the subsequent quark scattering, which was found to control induced gluon emission in finite non-Abelian plasmas [3, 10, 11]. Inverse Compton scattering in the QGP [12] has also been suggested as the dominant source of intermediate p_T photons if the γ acquires most of the momentum of the incoming quark. Such enhancement effects, in conjunction with their associated negative azimuthal asymmetry coefficient $v_2(p_T)$ [8, 13], do not appear to be compatible with existing direct photon data at RHIC [2, 14, 15].

Recent phenomenological refinements [16, 17] suggest that the QGP enhancement of direct γ production may be smaller than previously expected and partly cancelled by the quenching of fragmentation photons. Still, there is no calculation to date that consistently includes known nuclear matter effects, such as the Cronin effect [18, 19, 20], shadowing [21, 22], and cold nuclear matter energy loss [23], to provide quantitative guidance for the relative strength of initial- and final-state modifications in the observed γ cross sections. An additional serious deficiency in the theory and phenomenology of direct photon production in heavy ion collisions is the absence of systematic studies in proton-nucleus (p+A) and nucleus-nucleus (A+A) collisions for different system sizes and center of mass energies. This is especially true now, when new experimental results from RHIC are soon expected to become available [14, 24]. Last but not least, only through extensive detailed comparison between theory and data [5] can one test the model validity and gain confidence in the extracted quantitative properties [25] of the dense matter created in heavy ion reactions.

With this motivation, we derive the QGP-induced γ spectrum for hard quark production in finite size plasmas. The same model of jet-medium interactions is used to calculate the quark conversion cross section and the suppression of fragmentation photons. These theoretical results, when applicable, are combined in a numerical simulation with cold nuclear matter effects to provide model predictions for d+Cu, d+Au, Cu+Cu and Au+Au reactions at center of mass energies of 62.4 GeV and 200 GeV per nucleon pair at RHIC. This article is organized as follows: in section II we highlight the differences between gluon and photon bremsstrahlung and identify the theoretical approach that reproduces the known Bethe-Heitler spectrum. The derivation of the final-state medium-induced photon radiation in the reaction operator approach is given in section III. Numerical results, relevant to the phenomenology of direct γ production are also shown. In section IV we carry out a systematic investigation of cold and hot nuclear matter effects that alter the mid-rapidity photon cross section in ultra-relativistic collisions of heavy nuclei at RHIC. A summary and conclusions are presented in section V.

II. PHOTON VERSUS GLUON BREMSSTRAHLUNG

The computation of photon bremsstrahlung is usually considered to be easier than that of gluon bremsstrahlung due to the absence of self-interactions of the gauge boson. However, it is not well appreciated that the two physics processes are quite different. To illustrate this, we first examine the radiative amplitude that corresponds to the case of single scattering of a fast on-shell quark [10, 26]:

$$\mathcal{M}_{rad}(k) \propto 2ig_s\epsilon_\perp \cdot \left(\frac{\mathbf{k}_\perp}{\mathbf{k}_\perp^2} - \frac{(\mathbf{k}-\mathbf{q})_\perp}{(\mathbf{k}-\mathbf{q})_\perp^2}\right) e^{i\frac{\mathbf{k}_\perp^2}{2k^+}z^+}[T^c, T^a] \,. \tag{1}$$

In Eq. (1) g_s is the strong coupling constant, $k^\mu = [k^+, k^-, \mathbf{k}_\perp]$ is the momentum of the radiated gluon in light-cone coordinates and ϵ is its polarization vector. We denote by $q^\mu = [q^+ = 0, q^-, \mathbf{q}_\perp]$ the momentum exchange with the medium at position z and by $T^c, T^a \in \mathrm{SU}(3)$ the color matrices at the emission and interaction vertexes. Evidently, it is the color rotation of the parent parton and the re-interaction of the bremsstrahlung gluon in nuclear matter that determine the gluon emission intensity and allow neglect of the deflection of the jet. If we, however, take the Quantum Electro-Dynamics (QED) limit $g_s \to e_q = (\pm 1/3, \pm 2/3)e$, $T_c \to \mathbf{1}$ in Eq. (1) we find $\mathcal{M}^{\gamma}_{rad}(k) \to 0$. Therefore, a theoretical approach developed to describe gluon emission cannot be directly generalized to photon emission and vice versa [27]. Our conclusion is independent of the specific example of incoherent parton scattering. All regimes of coherent inelastic scattering can be treated in the unified framework of the reaction operator approach [23]. The reaction operator $\hat{R}_n$ describes the effect of one additional correlated in-medium scattering at position z_n at the cross section level and is process dependent. Taking the above mentioned QED limit of $\hat{R}_n$ derived for gluon bremsstrahlung [10], one finds:

$$\hat{R}_n = T_a T_a - (C_F/2)\mathbf{1} - (C_F/2)\mathbf{1} \equiv \mathbf{0} \,. \tag{2}$$

In Eq. (2) C_F is the quadratic Casimir in the fundamental representation of SU(3). Thus, better treatment of jet-medium interactions is needed for both incoherent and coherent photon emission calculations.

With these results in mind, we first identify the refinement of the kinematic approximations necessary to derive the induced γ spectrum. The scattering of a fast quark in nuclear matter is modelled via interactions with an external non-Abelian field $V^{\mu,c}(q)$ [18]:

$$\begin{aligned} V^{\mu,c}(q) &= n^\mu \, 2\pi\delta(q^+) \, V^c(q) \, e^{iq\cdot z} \,, \\ g_s V^c(q) &\equiv v(q) \, T^c(t) \,. \end{aligned} \tag{3}$$

Here, the four-vector $n^\mu = \delta^{\mu,-} = [0, 1, \mathbf{0}_\perp]$ and the color matrix $T^c(t) \in \mathrm{SU}_c(3)$ in Eq.(3) represents the target charge that creates the non-Abelian field. We take the Fourier transform $v(q)$ to be of color-screened Yukawa type but with Lorentz boost invariance:

$$v(q) \equiv \frac{4\pi\alpha_s}{-q^{\,2} + \mu^2} = \frac{4\pi\alpha_s}{\mathbf{q}_\perp^{\,2} + \mu^2} = v(\mathbf{q}_\perp) \;, \tag{4}$$

where we have used the $q^+ = 0$ choice of frame. This specific form of $v(q) = v(\mathbf{q}_\perp)$ is particularly useful since in-medium interactions in both hot and cold nuclear matter are of finite range $r_{int.} = \mu^{-1}$ and we shall assume that $\lambda_q \mu \gg 1$, where λ is the quark mean free path.

The differential photon bremsstrahlung spectrum arises from single-Born scattering diagrams shown in the top panel of Fig. 1. Using a high energy approximation for the quark to simplify the interaction and emission vertexes we obtain:

$$\begin{aligned} i\mathcal{M}^D_{RHS}(k) &= \int \frac{d^4q}{(2\pi)^4}(-ie)\frac{i\epsilon^\mu(2p_f+k)_\mu}{(p_f+k)^2+i\epsilon} \\ &\quad \times (-ig_sT^c(p))\frac{iV^{\nu,c}(q)(2p_f+2k-q)_\nu}{(p_f+k-q)^2+i\epsilon} \\ &\approx \left[-i\int\frac{d^2\mathbf{q}_\perp}{(2\pi)^2}v(\mathbf{q}_\perp)e^{-i\mathbf{q}_\perp\cdot\mathbf{z}_\perp}T^c(p)T^c(t)\right] \\ &\quad \times e\left(\frac{\epsilon\cdot p_f}{k\cdot p_f}\right)e^{iz^+k^-} \,. \end{aligned} \tag{5}$$

For the second γ emission diagram similar considerations lead to:

$$\begin{aligned} i\mathcal{M}^D_{LHS}(k) &\approx \left[-i\int\frac{d^2\mathbf{q}_\perp}{(2\pi)^2}v(\mathbf{q}_\perp)e^{-i\mathbf{q}_\perp\cdot\mathbf{z}_\perp}T^c(p)T^c(t)\right] \\ &\quad \times e\left(-\frac{\epsilon\cdot p_i}{k\cdot p_i}\right)e^{iz^+k^-} \,, \end{aligned} \tag{6}$$

and the radiative matrix element at position z_i reads:

$$\mathcal{M}_{rad}(k,\{i\}) = e\left(\frac{\epsilon\cdot p_f}{k\cdot p_f} - \frac{\epsilon\cdot p_i}{k\cdot p_i}\right)e^{iz_i^+k^-} \,. \tag{7}$$

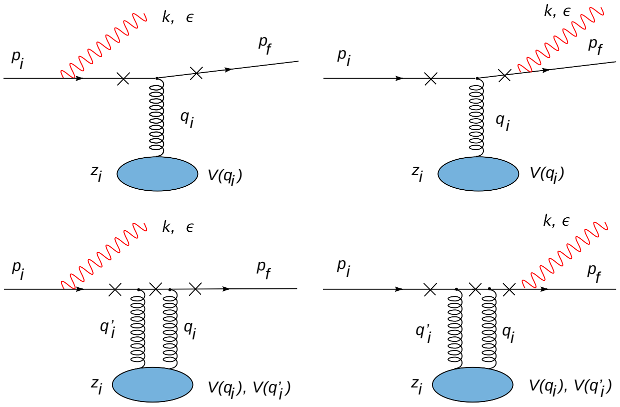

FIG. 1: Top panel: single-Born diagrams for medium-induced γ emission. Bottom panel: the corresponding double-Born diagrams in the $z_{i'} \to z_i$ limit. The third diagram, known to vanish in this limit [10], is not shown. We denote by " $\times$" the propagators that enter the calculation.

In Eq. (7) the collisional amplitude is not shown. Let the initial- and final-state momenta of a fast on-shell quark be $p_i = [E^+, Q^2_{\perp\, i-1}/(2E^+), \mathbf{Q}_{\perp\, i-1}]$, $p_f = [E^+, Q^2_{\perp\, i}/(2E^+), \mathbf{Q}_{\perp\, i}]$, such that $\mathbf{Q}_{\perp\, i} - \mathbf{Q}_{\perp\, i-1} = \mathbf{q}_{\perp\, i}$. The double differential medium-induced photon distribution is then given by:

$$k^+ \frac{dN^\gamma(k;\{i\})}{dk^+ d^2\mathbf{k}_\perp} = \frac{1}{2(2\pi)^3} |\mathcal{M}_{rad}(k,\{i\})|^2$$
$$= \frac{\alpha_{em}}{\pi^2} \frac{\left(\frac{k^+}{E^+}\right)^2 \mathbf{q}^2_{\perp\, i}}{\left(\mathbf{k}_\perp - \frac{k^+}{E^+}\mathbf{Q}_{\perp\, i-1}\right)^2 \left(\mathbf{k}_\perp - \frac{k^+}{E^+}\mathbf{Q}_{\perp\, i}\right)^2} , \quad (8)$$

and is dominated by emission coincident with the directions of the incoming and the outgoing quarks. Changing variables $\kappa = \mathbf{k}_\perp - \mathbf{k}^{(\mathrm{pole})}_\perp$, $\mathbf{k}^{(\mathrm{pole})}_\perp = \mathbf{Q}_{\perp\, i} k^+/E^+, \mathbf{Q}_{\perp\, i-1} k^+/E^+$, respectively, we obtain the QED double logarithmic result:

$$N^\gamma(\{i\}) \approx 2\frac{\alpha_{em}}{\pi} \ln \frac{k^+_{\mathrm{max}}}{k^+_{\mathrm{min}}} \ln \frac{q^2_{\mathrm{max}}}{m^2} , \quad (9)$$

where m^2 regulates the collinear divergence.

In the case of coherent gluon emission in finite media with few subsequent scatterings, the interference between the hard (vacuum) and soft (medium-induced) bremsstrahlung largely determines the LPM cancellation pattern [3, 10]. Double-Born diagrams, with two momentum exchanges at the same position $z_i = z'_i$, can contribute at any fixed order in opacity. The relevant double-Born diagrams for photon emission are shown in the bottom panel of Fig. 1. We find:

$$\begin{aligned} i\mathcal{M}^V_{RHS}(k) &= \int \frac{d^4q}{(2\pi)^4} \frac{d^4q'}{(2\pi)^4} (-ie) \frac{i\epsilon^\mu(2p_f+k)_\mu}{(p_f+k)^2 + i\epsilon} \\ &\times\ (-ig_s T^c(p)) \frac{iV^{\nu,c}(q)(2p_f+2k-q)_\nu}{(p_f+k-q)^2+i\epsilon} \\ &\times\ (-ig_s T^d(p)) \frac{iV^{\delta,d}(q')(2p_f+2k-2q-q')_\delta}{(p_f+k-q-q')^2+i\epsilon} \\ &\approx\ \frac{1}{A_\perp}\left[-\frac{1}{2}\int \frac{d^2\mathbf{q}_\perp}{(2\pi)^2} |v(\mathbf{q}_\perp)|^2 \frac{C_t C_p}{d_A}\right] \\ &\quad \times e \left(\frac{\epsilon\cdot p_f}{k\cdot p_f}\right) e^{iz^+k^-} \ . \end{aligned} \quad (10)$$

To obtain the result in Eq. (10) we averaged over the initial and summed over the final parton colors. We also carried out the average over the position of the scattering center in the transverse plane: $A_\perp^{-1}\int d^2\mathbf{z}_\perp \exp[-i\mathbf{z}_\perp\cdot(\mathbf{q}_\perp + \mathbf{q}'_\perp)] = A_\perp^{-1}(2\pi)^2\delta^2(\mathbf{q}_\perp + \mathbf{q}'_\perp)$. For single-Born interactions, see Eqs. (5) and (6), such averages are possible only after squaring the amplitudes. The result differs from the one for virtual interactions in yielding $\delta^2(\mathbf{q}_\perp - \mathbf{q}'_\perp)$, and in the absence of the factor $-1/2$, which accompanies the collision term.

Similarly, for the second virtual diagram in Fig. 1 we obtain:

$$\begin{aligned} i\mathcal{M}^V_{LHS}(k) &\approx \frac{1}{A_\perp}\left[-\frac{1}{2}\int \frac{d^2\mathbf{q}_\perp}{(2\pi)^2} |v(\mathbf{q}_\perp)|^2 \frac{C_t C_p}{d_A}\right] \\ &\quad \times e \left(-\frac{\epsilon\cdot p_i}{k\cdot p_i}\right) e^{iz^+k^-} \ . \end{aligned} \quad (11)$$

Adding Eqs. (10) and (11) we see that the same general radiation matrix element, Eq. (7), can be factorized for double-Born interactions. In Eqs. (10) and (11) $d\sigma^{\mathrm{el}}/d^2\mathbf{q}_\perp = (C_t C_p/d_A)|v(\mathbf{q}_\perp|^2/(2\pi)^2$ is the differential scattering cross section, calculated in the Born approximation. However, $\mathbf{q}_\perp + \mathbf{q}'_\perp = 0$, and $p_i = p_f$ implies that the double-Born interaction does not contribute a new photon bremsstrahlung amplitude.

III. DIFFERENTIAL PHOTON BREMSSTRAHLUNG SPECTRUM TO ALL ORDERS IN OPACITY

To define the iterative procedure of computing the photon bremsstrahlung contribution from multiple scattering, we first consider the action of the direct operator $\hat{D}_n$ at position z_n on a radiative amplitude with $n-1$ correlated scatterings. In what follows we have dropped the collisional amplitudes since they were shown to yield an elastic scattering cross section per order in opacity for both diffusion [18, 28] and radiative [10] processes. The result of such action can be represented as:

$$\begin{aligned} \hat{D}_n \mathcal{M}^{rad}_{i_1\cdots i_{n-1}}(k) &\equiv (\hat{1} + \hat{B}_n)\mathcal{M}^{rad}_{i_1\cdots i_{n-1}}(k) \\ &= \mathcal{M}^{rad}_{i_1\cdots i_{n-1}}(k) + \left(-\tfrac{1}{2}\right)^{N_v(\mathcal{M}^{rad}_{i_1\cdots i_{n-1}})} \mathcal{M}_{rad}(k,\{n\}) \ . \end{aligned} \quad (12)$$

Here, the factor $\left(-\frac{1}{2}\right)^{N_v}$ arises because every virtual contact interaction in the amplitude gives a factor $-\frac{1}{2}$, and $N_v(\mathcal{M}^{rad}_{i_1\cdots i_{n-1}})$ is their number. The first term in Eq. (12) corresponds to a momentum exchange with the energetic jet. In the high energy limit we do not keep track of the transverse modification of the parent parton except for the contribution to the soft photon bremsstrahlung. This approximation does not affect the calculation of the intensity spectrum dI^γ/dk^+ but the angular distribution must be convoluted with the medium-induced jet acoplanarity, which we here neglect. The second term in Eq. (12) is the new radiative contribution, Eq. (7), at position z_n, and the prefactor accounts for the number of preceding virtual interactions in the amplitude. Next, we consider the double-Born interaction of the quark at position z_n. From section II we know that there is no new γ bremsstrahlung contribution since $p_f = p_i$. However, a factor $-1/2$ arises for the forward elastic scattering. The modification of the amplitude $\mathcal{M}^{rad}_{i_1\cdots i_{n-1}}(k)$ is found to be:

$$\hat{V}_n \mathcal{M}^{rad}_{i_1\cdots i_{n-1}}(k) = -\frac{1}{2}\mathcal{M}^{rad}_{i_1\cdots i_{n-1}}(k) \ . \quad (13)$$

In both Eq. (12) and Eq. (13) we have omitted the color factors since for the simple case of individual parton propagation these are trivially absorbed in the elastic scattering cross section or inverse mean free path per order in opacity [18].

Let $i_n = 0, 1, 2$ indicate for each n: no interaction, direct interaction and virtual interaction with the medium, respectively [10]. Expansion in powers of $\sigma^{\rm el}$ or, equivalently, $1/\lambda_q$ requires that in the conjugate amplitude $\bar{\mathcal{M}}_{rad}^{i_1\cdots i_n}(k)$ we have $\bar{i_n} = 2 - i_n$. Consequently, the contribution to the radiation pattern at n-th order in opacity is:

$$
\begin{aligned}
dN^\gamma(k,n) &\propto \sum_{i_1\cdots i_n=0}^{2} \bar{\mathcal{M}}_{rad}^{i_1\cdots i_n}(k)\mathcal{M}^{rad}_{i_1\cdots i_n}(k) \\
&= \sum_{i_1\cdots i_{n-1}=0}^{2} \bar{\mathcal{M}}_{rad}^{i_1\cdots i_{n-1}}(k)(\hat{D}^\dagger\hat{D}+\hat{V}^\dagger+\hat{V})\mathcal{M}^{rad}_{i_1\cdots i_{n-1}}(k) \\
&= \sum_{i_1\cdots i_{n-1}=0}^{2} \bar{\mathcal{M}}_{rad}^{i_1\cdots i_{n-1}}(k)(\hat{B}_n^\dagger\hat{B}_n+\hat{B}_n^\dagger+\hat{B}_n)\mathcal{M}^{rad}_{i_1\cdots i_{n-1}}(k) \ .
\end{aligned}
\tag{14}
$$

For medium induced photon emission, the reaction operator $\hat{R}_n = \hat{D}_n^\dagger\hat{D}_n + \hat{V}_n^\dagger + \hat{V}_n = \hat{B}_n^\dagger\hat{B}_n + \hat{B}_n^\dagger + \hat{B}_n$ has a particularly simple form. The first term in Eq. (14) vanishes beyond first order ($n = 1$) in opacity [10]:

$$
\begin{aligned}
&\sum_{i_1\cdots i_{n-1}=0}^{2} \bar{\mathcal{M}}_{rad}^{i_1\cdots i_{n-1}}(k)\hat{B}_n^\dagger\hat{B}_n\bar{\mathcal{M}}_{rad}^{i_1\cdots i_{n-1}}(k) \\
&= |\mathcal{M}_{rad}(k,\{n\})|^2 \sum_{i_1\cdots i_{n-1}=0}^{2} \left(-\tfrac{1}{2}\right)^{\bar{N}_v}\left(-\tfrac{1}{2}\right)^{N_v} = 0 \ ,
\end{aligned}
\tag{15}
$$

where we have used $\left(-\frac{1}{2}-\frac{1}{2}+1\right)^{n-1} = 0$ for $n \geq 2$ [10]. The 2nd and 3rd terms in Eq. (14) yield:

$$
\begin{aligned}
&2Re\,\mathcal{M}^*_{rad}(k,\{n\}) \sum_{i_1\cdots i_{n-1}=0}^{2} \left(-\tfrac{1}{2}\right)^{\bar{N}_v} \bar{\mathcal{M}}_{rad}^{i_1\cdots i_{n-1}}(k) \\
&= \ 2Re\,\mathcal{M}^*_{rad}(k,\{n\})\mathcal{M}_{rad}(k,\{n-1\}) \\
&\quad \times \sum_{i_1\cdots i_{n-2}=0}^{2} \left(-\tfrac{1}{2}\right)^{\bar{N}_v}\left(-\tfrac{1}{2}\right)^{N_v} = 0 \ ,
\end{aligned}
\tag{16}
$$

if $n \geq 3$. Therefore, unlike the case of gluon bremsstrahlung, photon bremsstrahlung contributions vanish beyond second order in opacity.

Taking into account the interactions of the parent quark along its trajectory through the QGP and the average over the transverse momentum transfers, the main theoretical result derived in this letter reads:

$$
\begin{aligned}
k^+\frac{dN^\gamma(k)}{dk^+d^2\mathbf{k}_\perp} &= \frac{\alpha_{em}}{\pi^2}\Bigg\{ \int \frac{d\Delta z_1}{\lambda_q(z_1)} \int d^2\mathbf{q}_{\perp\,1} \frac{1}{\sigma^{\rm el}} \frac{d^2\sigma^{\rm el}}{d^2\mathbf{q}_{\perp\,1}} \\
&\times \left[|\mathcal{M}_{rad}(\{1\})|^2 + 2\mathcal{M}^*_{rad}(\{1\})\mathcal{M}_{rad}(\{0\})\cos(k^-\Delta z_1^+)\right] \\
&+ \prod_{i=1}^{2}\left[\int \frac{d\Delta z_i}{\lambda_q(z_i)} \int d^2\mathbf{q}_{\perp\,i} \frac{1}{\sigma^{\rm el}} \frac{d^2\sigma^{\rm el}}{d^2\mathbf{q}_{\perp\,i}}\right] \\
&\times 2\mathcal{M}^*_{rad}(\{2\})\mathcal{M}^*_{rad}(\{1\})\cos(k^-\Delta z_2^+)\Bigg\} \ .
\end{aligned}
\tag{17}
$$

In Eq. (17) $\Delta z_i^+ = z_i^+ - z_{i-1}^+$, the Δz_i integrals are nested, and $\tau_f^{-1} = \mathbf{k}^2/(2\omega) \approx \sqrt{2}\,k^-$ is the inverse photon formation time. When $\tau_f^{-1}\lambda_q \gg 1$ the photons decohere early from the parent quark and our result reduces to incoherent emission from individual scattering centers. Our result differs from previous findings [7, 9] in several important ways: first, it treats the case of finite $L/\lambda_q \sim$ few, relevant to heavy ion physics. Second, we find that the most significant contribution to the LPM effect for photons comes from the interference of the medium-induced photon radiation with the hard emission from the large Q^2 scattering of the parent quark. Finally, we find that there can be non-linear corrections $\sim L^2$ to the dominant linear in L behavior of the photon spectrum. Note that calculations of final-state γ emission have also been carried out in deep inelastic scattering on nuclei [27, 29] using the high twist approach [11].

We are now ready to study numerically the final-state QGP-induced photon spectrum. Our results are limited to first order in opacity. The question of whether destructive interference may even cancel part of the hard photon bremsstrahlung is deferred for future studies. With Eq. (7) representing the amplitude of both light and heavy fermions, the intensity spectrum is easily generalized to quarks with physical and thermal mass, $m^2 = M_q^2 + C_F g_s^2 T^2/4$. Notable differences from the $m = 0$ case include regulation of the poles in Eq. (8) via $(k^+/E^+)^2 m^2$, appearance of new terms $\propto m^2$, and finite quark velocity, $\beta < 1$. We show an example of a quark propagating outwards from the center of the medium created in $b = 3$ fm Au+Au collisions at RHIC. For a typical integrated gluon rapidity density, $dN^g/dy \simeq 1150$, distributed proportional to the 2D participant number density $dN_{\rm part}/d^2\mathbf{x}_\perp$, we calculate the temperature $T(\mathbf{x}_\perp, t)$ as a function of time and position in the transverse plane, assuming approximate Bjorken expansion of the QGP near midrapidity $y = 0$. The necessary Debye screening scale $\mu(T) = m_D(T) = g_s T$, elastic scattering cross section $\sigma^{qg}(T)$, and quark mean free path $\lambda_q(T) = 1/\sigma^{qg}(T)\rho(T)$ are evaluated as in [4] with $g_s = 2.5$. The top panel of Fig. 2 shows the medium-induced photon number spectrum $d\bar{N}^\gamma/dx = (e/e_q)^2 dN^\gamma/dx$, $x = k^+/E^+$, normalized by the squared fractional quark electric charge (bar will denote such scaling for any physics quantity). We considered light, $M_{u,d} = 0$ GeV, and heavy, $M_c = 1.5$ GeV, $M_b = 4.5$ GeV, quarks of energy $E_q = 100$ GeV in the Bethe-Heitler limit and to first

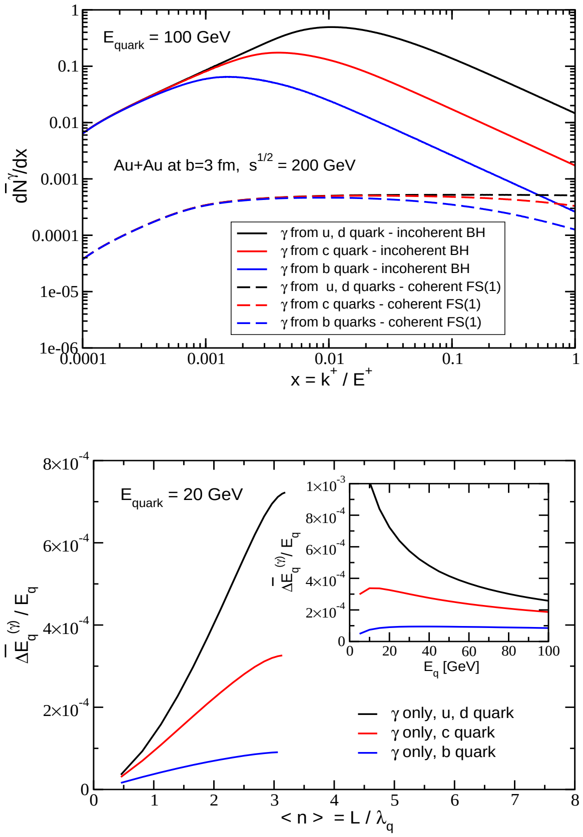

FIG. 2: Top panel: medium-induced photon number spectrum versus $x = k^+/E^+$ for $E_q = 100$ GeV light, charm and bottom quarks in central Au+Au collisions at $\sqrt{s} = 200$ GeV. Both the incoherent Bethe-Heitler (solid) and the coherent final-state (dashed) bremsstrahlung cases are shown. Bottom panel: partial fractional quark energy loss $\Delta E_q^{(\gamma)}/E_q$ due to γ emission versus the mean number of quark interactions $\langle n \rangle = L/\lambda_q$. Insert illustrates the energy dependence of $\Delta E_q^{(\gamma)}/E_q$.

order in opacity. In the absence of coherence, the induced γ spectrum is dominated by photon energies $\omega \sim$ a few $\times T$. The contributions of the heavy quark sector to the medium-induced photon multiplicity and the energy loss due to photon emission are strongly suppressed. When the interference between the vacuum and the medium-induced photon radiation is taken into account, we find that the spectrum dN^γ/dx is suppressed much more effectively than in the limit of very large number of soft scatterings for on-shell quarks [9]. The bottom panel of Fig. 2 shows the dependence of the partial fractional energy loss due to γ emission versus the mean number of quark interactions in the QGP:

$$\langle n \rangle = L/\lambda_q = \int dz/\lambda_q(z) \; . \qquad (18)$$

We note that for light and moderately heavy quarks, such as the charm quark, there is clear non-linear dependence of $\Delta E_q^{(\gamma)}/E_q$ on $\langle n \rangle$. It is correlated with deviations from the naive expectation, $\Delta E_q^{(\gamma)} \propto E_q$, as illustrated in the insert in Fig. 2. Medium-induced photon emission in both the coherent and incoherent limits is too small, $\Delta E_q^{(\gamma)}/E_q < 1\%$, to contribute to the quenching of quark jets. Last but not least, we emphasize that the number of interactions in the QGP, even for jets emerging from the center of the heavy ion collision region, is small, $\langle n \rangle = 3.1$. As in the case of gluon emission, this is a clear indication that, even in the most central Au+Au reactions at RHIC, we are *not* in the limit of large number of scatterings. For consistency with the calculation of light hadron attenuation, in our numerical estimates we use an effective geometry of $L = 6$ fm and uniform distribution of partons [4]. In this case $\langle n \rangle$ is reduced to 2.4, accounting for jets close to the periphery of the interaction region.

IV. PHENOMENOLOGY OF HARD PHOTON PRODUCTION IN P+A AND A+A COLLISIONS

With the results from the previous section at hand, we now turn to the question of hard, $p_T >$ a few GeV, photon production in heavy-ion collisions. QGP and cold nuclear matter effects are identified through the nuclear modification ratio:

$$R_{AB}(p_T, b) = \frac{d\sigma_{AB}}{dyd^2\mathbf{p}_T} \bigg/ N_{AB}^{\rm coll}(b) \frac{d\sigma_{pp}}{dyd^2\mathbf{p}_T} \; , \qquad (19)$$

where the number of binary collisions, $N_{AB}^{\rm coll}(b)$ in Eq. (19), is computed in an optical Glauber model. The baseline p+p cross section is evaluated in factorized perturbative QCD to lowest order and leading twist as fol-

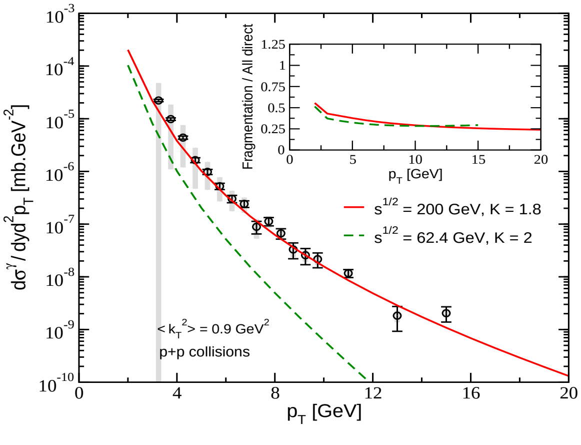

FIG. 3: Direct photon production cross section in p+p collisions at $\sqrt{s} = 62.4$ GeV and 200 GeV. Data at the higher RHIC energy is from PHENIX [34]. Insert shows the fraction of fragmentation to all direct photons.

lows:

$$\begin{aligned}\frac{d\sigma^{\gamma}_{pp}}{dy d^2\mathbf{p}_T} &= K\sum_{abcd}\int dy_d \int d^2\mathbf{k}_a d^2\mathbf{k}_b\, \frac{f(k_b)f(k_b)}{|J(k_a,k_b)|} \\ &\quad\times \int \frac{dz}{z^2}\, D_{\gamma/c}(z,\mu_{fr})\, \frac{\alpha_s(\mu_r)\alpha_c}{2S}|\overline{M}_{ab\to cd}|^2 \\ &\quad\times \frac{\phi_{a/N}(x_a,\mu_f)\phi_{b/N}(x_b,\mu_f)}{x_a x_b} \ . \qquad (20)\end{aligned}$$

In Eq. (20) we adhere to the standard notation, see for example [4, 21, 33], and the Jacobian reads:

$$J_{x_a,x_b}(k_a,k_b) = \frac{S}{2}\left(1 - \frac{k_a^2 k_b^2}{x_a^2 S x_b^2 S}\right) \ , \qquad (21)$$

subject to the hard scattering constraint $k_{a,b} < x_{a,b}\sqrt{S}$. In elementary p+p collisions we use $\langle k^2_{a,b}\rangle = 0.9$ GeV^2 for the normalized Gaussian parton transverse momentum distributions, $f(k_{a,b})$, and phenomenological K-factors cancel in $R_{AB}(p_T)$. One observes that Eq. (20) includes both prompt photons, $c = \gamma$, $\alpha_c = \alpha_{em} = 1/137.036$, $D_{\gamma/\gamma}(z) = \delta(1-z)$, and fragmentation photons, $c = q, \bar{q}, g$, $\alpha_c = \alpha_s(\mu_r)$, with $D_{\gamma/c}(z,\mu_{fr})$ taken from Ref. [33]. Figure 3 shows the cross sections for direct γ production in p+p collisions at $\sqrt{s} = 62.4$ GeV and 200 GeV and identifies the fragmentation fraction of direct photons that will undergo final-state modification in the QGP.

The first and necessary step, that has thus far been neglected in direct photon phenomenology, is a systematic study of nuclear effects in p+A reactions. Not only do the isospin effect, Cronin effect, shadowing, and energy loss in nuclei significantly affect the observable $R_{AA}(p_T)$, but these are interesting in their own right in light of the current and future d+Au measurements at RHIC [24]. Theoretical approaches to the Cronin effect are well documented [19] and are centered around the idea of initial-state multiple scattering [20]. In our calculations the Cronin effect in the nuclear medium is controlled by the broadening of the transverse momenta of incoming partons as follows:

$$\begin{aligned}\langle k_T^2\rangle &= \langle k_T^2\rangle_{pp} + \langle k_T^2\rangle_{med} \ , \\ \langle k_T^2\rangle_{med} &= \left(\frac{2\mu^2 L}{\lambda}\right)_{q,g} \times \max[1, \ln(1+\delta\, p_T^2)] \ , \qquad (22)\end{aligned}$$

where the term $\ln(1+\delta\, p_T^2)$ takes into account the power law tail of the k_T distribution beyond the naive Gaussian random walk [30] (e.g. Moliere multiple scattering). Specifically, $\mu^2 = 0.12$ GeV^2, $\lambda_g = (C_F/C_A)\lambda_q = 1$ fm and $\delta = 0.3$ are fixed to reproduce the experimental p+A data when we include initial-state energy loss and are compatible with our earlier findings for $\langle k_T^2\rangle_{med}$ within 20% [20, 30]. In Eq. (22) L gives the length of the nuclear medium. We note that in semi-inclusive deep inelastic scattering (SIDIS) the final-state broadening is expected to be approximately equal to the initial-state diffusion in k_T. A naive estimate of the medium-induced contribution to the hadron $\langle \Delta p_T^2\rangle_A = \langle p_T^2\rangle_A - \langle p_T^2\rangle_D$ can be made from Eq. (22). The numerical results at leading order for $Q^2 = 5$ GeV^2, $\langle \Delta p_T^2\rangle_{Ne} = 0.14$ GeV^2 $\langle \Delta p_T^2\rangle_{Kr} = 0.29$ GeV^2 and $\langle \Delta p_T^2\rangle_{Xe} = 0.36$ GeV^2, are compatible within error bars with recent preliminary HERMES data [31].

In this work, only the EMC effect was parametrized [22] and shadowing was calculated from the coherent final-state parton interactions [21]. The only parameter, the scale of power corrections ξ^2 [21], is constrained by the mean squared momentum transfer per unit length μ^2/λ so that $(\xi^2 A^{1/3})_{q,g} \approx (2\mu^2 L/\lambda)_{q,g}$ in minimum bias reactions, which yields $(\xi^2)_q \approx 0.12$ GeV^2. Cold nuclear matter energy loss [23] was consistently calculated with the same lengths, momentum transfers and mean free paths as in Eq. (22) and incorporated in the pQCD calculation as follows:

$$\begin{aligned}\phi_{a,b/N}(x_{a,b},Q^2) &\to \phi_{a,b/N}\left(\frac{x_{a,b}}{1-\epsilon_{a,b}}, Q^2\right) \\ &\approx \phi_{a,b/N}\left(x_{a,b}(1+\epsilon_{a,b}), Q^2\right) \ , \qquad (23)\end{aligned}$$

when $\epsilon_{a,b} \ll 1$. Here, $\epsilon_{a,b}$ are the fractional energy losses for the incoming partons a, b evaluated in the rest frame of the corresponding target nucleus. It has been shown for the typical hot QGP created at RHIC that the effect of multi-gluon fluctuations of the induced bremsstrahlung on the quenching of jets could be mimicked by a simple reduction of the mean energy loss $\epsilon_{eff} = \kappa\, \Delta E/E$, where $\kappa = 0.4 - 0.5$ [32]. Though fluctuations of the initial-state cold nuclear matter energy loss have not yet been studied, in our calculations we make a similar approximation. We note that the weaker falloff with energy of the incoming parton flux, when compared to the hard scattered (additional $\sim 1/p_T^4$) final-state quark and gluon distributions, implies values of κ closer to unity. The specific choice that we make, $\kappa = 0.7$, was constrained through the evaluation of the π^0 production cross section in Cu+Cu collisions at RHIC [5] which provided a good description of the experimental data.

Our results for minimum-bias d+Au (solid lines) and d+Cu (dashed lines) collisions are shown in Fig. 4. The calculated $R_{dA}(p_T)$ at $\sqrt{s} = 200$ GeV and 62.4 GeV are presented in the top and bottom panels, respectively. In the $p_T < 5 - 7$ GeV region, the nuclear modification is dominated by Cronin enhancement with a magnitude that is not strongly affected by shadowing but is sensitive to the initial-state energy loss. The complementary $p_T > 5 - 7$ GeV part of phase space is characterized by $R_{dA}(p_T) < 1$ with the isospin effect, included in all calculations, being one of the major contributors. The EMC effect only becomes noticeable at the lower C.M. energy and at the highest transverse momenta. Initial-state, cold nuclear matter energy loss can contribute as much as the isospin effect at high p_T. We emphasize that, at transverse momenta ~ 15 GeV, nuclear effects on the direct photon cross section can be as large as 20% at $\sqrt{s} = 200$ GeV and 40% at $\sqrt{s} = 62.4$ GeV in minimum

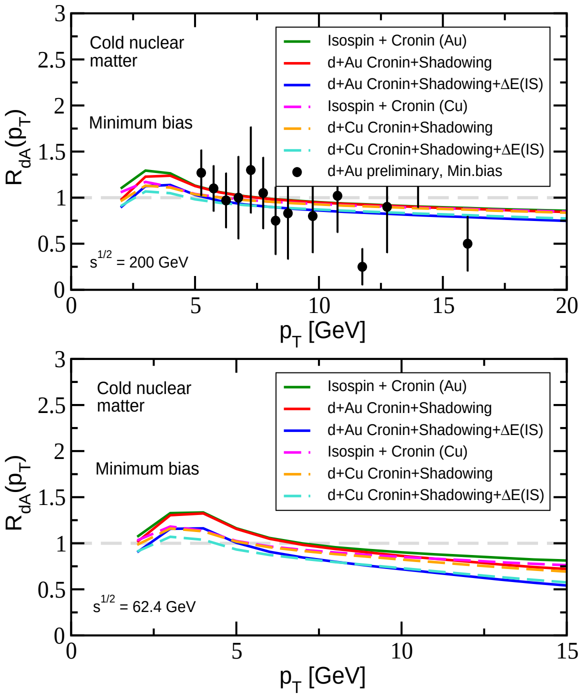

FIG. 4: Cold nuclear matter effects manifest in direct photon $R_{dAu}(p_T)$ in minimum bias d+Au (solid lines) and d+Cu (dashed lines) collisions. RHIC energies $\sqrt{s} = 62.4$ GeV and 200 GeV are shown in the top and bottom panels, respectively. Preliminary $\sqrt{s} = 200$ GeV minimum bias d+Au data is also included [24].

bias d+A collisions. Preliminary experimental data [24] is consistent with the theoretical expectation. However, given the large error bars, it cannot discriminate between different cold nuclear matter effects or constrain their magnitudes. Careful experimental investigation is needed to pinpoint these effects and, since they will be enhanced in A+A collisions, caution should be exercised in the interpretation of the $R^{\gamma}_{AA}(p_T)$ findings.

In A+A collisions, QGP-induced modification of direct photon production cross section includes competing effects: the quenching of fragmentation photons and the tree level (jet conversion) and bremsstrahlung photon enhancement. The quenching of fragmentation photons is modelled in the same way as the quenching of hadrons [20] and can be combined with the medium-induced γ contributions as follows:

$$D_{\gamma/c}(z) \;\Rightarrow\; \int_0^{1-z} d\epsilon \; P(\epsilon)\, \frac{1}{1-\epsilon} D_{\gamma/c}\left(\frac{z}{1-\epsilon}\right) + \frac{dN^{\gamma}_{\rm med.}(c)}{dz} + N^{\gamma}_{\rm conv.}(c)\delta(1-z) \; . \quad (24)$$

Here, $P(\epsilon)$ is the probability distribution of the fractional jet energy loss $\epsilon = \Delta E/E$ [4, 32], $dN^{\gamma}_{\rm med.}(c)/dz$ is the QGP-induced bremsstrahlung that we calculated in section II, and $N^{\gamma}_{\rm conv.}(c)$ is the number of jets converted to photons. For such conversions, in Eq. (24) the $p_\gamma \approx p_c$ approximation [12] that stems from the limit of small t-channel momentum transfers to energetic jets is implicit. For a parent quark propagating through the QGP:

$$N^{\gamma}_{\rm conv.}(c) = \int_{t_0}^{L} dt \; \rho(T) \sigma^{qg\to\gamma q}_{tot}(T) \; , \qquad (25)$$

where time and position dependence is taken via $T(\mathbf{x}_\perp, t)$. The cross section in Eq. (25), with $s \approx 2m_D E$ and $t \in (m_D^2, s/4)$, consistent with the forward scattering approximation, reads:

$$\sigma^{qg\to\gamma q} = \frac{\pi \alpha_s \alpha_{em}}{6 m_D E} \ln \frac{E}{2m_D} \; . \qquad (26)$$

Numerical results in central Au+Au and Cu+Cu collisions at the intermediate and top RHIC energies are shown in Fig. 5. The final-state gluon rapidity densities $dN^g/dy = 1150$ $(Au, 200\ \text{GeV})$, 800 $(Au, 62.4\ \text{GeV})$, 370 $(Cu, 200\ \text{GeV})$, 255 $(Cu, 62.4\ \text{GeV})$ are constrained by measured and extrapolated particle multiplicities at RHIC [4]. Of the final-state effects in the QGP, the left panels only include the quenching of fragmentation photons. Since a small fraction of the direct γ come from fragmentation processes and quark attenuation is significantly smaller, $\sim C_F/C_A$, when compared to gluon attenuation, the observable QGP modification is also very small. In fact, $R_{AA}(p_T)$ is dominated by cold nuclear matter effects, such as the ones shown in Fig. 4, amplified by the presence of two large nuclei. $R_{AA}(p_T)$ from published [1, 34] and preliminary [2, 14] data are shown for comparison. Given the error bars, only large Cronin enhancement at $\sqrt{s} = 62$ GeV is excluded, suggestive of the role of initial-state inelastic jet scattering in controlling the magnitude of the Cronin effect.

The right panels in Fig. 5 include the medium-induced photons and the jet conversion contribution. For completeness, we have also shown results for the incoherent Bethe-Heitler radiation spectrum and absence of initial state energy loss. This scenario gives direct γ enhancement as large as factors of 3 and 4 over the p+p baseline at $\sqrt{s} = 200$ GeV and 62 GeV, respectively. Not only is this case not supported theoretically by the results derived in this paper and in Ref. [23], but when compared to data, even with the present large experimental error bars, it is clearly excluded. In calculating the coherent final state photon emission rate, Eq. (17), and the jet conversion rate, Eq. (25), we also account for the time-dependent quenching of the quark as it propagates through the QGP:

$$R_{AA}(p_T, t) = (1 - f(t)) + R_{AA}(p_T) f(t) \; . \qquad (27)$$

Here, $R_{AA}(p_T)$ is the full final-state quark quenching, evaluated as in [4] for different system sizes and center of mass energies, and $f(t)$ interpolates between 0 and 1 to give the time dependence of radiative energy loss [23]. We find that this effect reduces $dN^{\gamma}_{\rm med}/dz$ and $N^{\gamma}_{\rm conv.}$ by $\sim 30\%$. Our results show that at transverse momenta

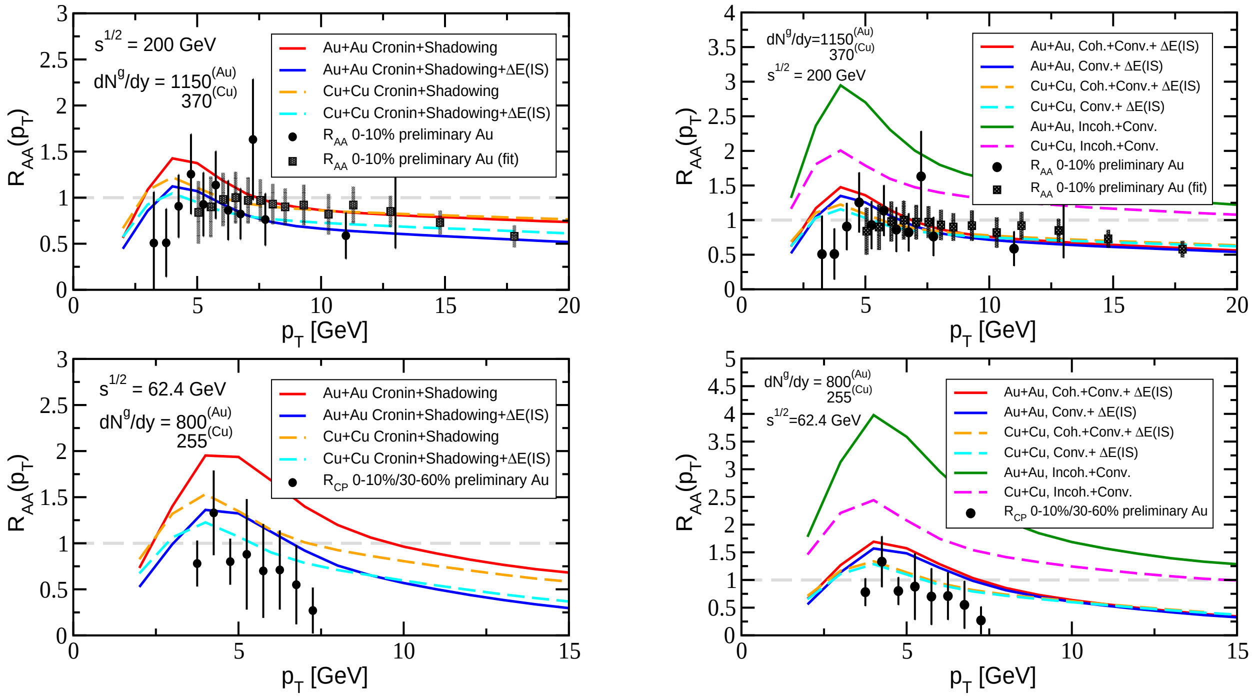

FIG. 5: Calculations of direct photon $R_{AA}(p_T)$ in central Au+Au (solid lines) and Cu+Cu (dashed lines) collisions. RHIC energies $\sqrt{s} = 62.4$ GeV and 200 GeV are shown in the top and bottom panels. Of the final-state QGP effects left panels only include the quenching of fragmentation photons. Right panels also include the jet conversion and medium-induced γ (both coherent and incoherent limits) enhancements. Preliminary $\sqrt{s} = 200$ GeV and 62.4 GeV Au+Au data is shown [2, 14]. At 200 GeV two preliminary $R_{AA}(p_T)$ results from [1, 34] (circles) and [14] (squares) are extracted.

$p_T < 5$ GeV the contribution from jet conversion to the total photon cross section is limited to $\sim 25\%$ and the contribution of medium-induced γ is limited to $\sim 10\%$. In the high p_T range the total enhancement contribution is found to be $\sim 5\%$.

V. CONCLUSIONS

In this paper, we provided a theoretical derivation of the final-state QGP-induced photon bremsstrahlung for the experimentally relevant case of hard jet production. We demonstrated that while the physics processes that control photon and gluon emission differ, the common Landau-Pomeranchuk-Migdal interference between the radiation from the hard scattering and the radiation from the subsequent soft quark interactions in the plasma leads to a significant suppression of the γ intensity. The photon spectrum was found to be attenuated at least by a factor of several for jet energies relevant for RHIC phenomenology, in contrast with the estimated modest 30% attenuation for asymptotic $t = -\infty$ on-shell jets in the limit of a very large number of soft interactions, where the interference with the bremsstrahlung that accompanies hard jet production has not been taken into account. We found that the suppression of dI^γ/dk^+ also leads to non-linear dependence of $\Delta E_q^\gamma(L/\lambda_q, E_q)$ on the system size and sub-linear dependence on the parent quark energy that have previously been associated primarily with gluon emission.

To help identify the significance of both cold and hot nuclear matter effects on direct photon production we carried out the first systematic phenomenological study of $R^\gamma_{AB}(p_T)$ in midrapidity d+Cu, d+Au, Cu+Cu and Au+Au reactions at RHIC energies of $\sqrt{s} = 62.4$ GeV and 200 GeV. As expected, in all cases we found that in the absence of QGP formation the nuclear modification factor at intermediate transverse momenta is dominated by the Cronin effect and at high transverse momenta by isospin effects and initial-state parton energy loss. Surprisingly, however, the contribution of final-state QGP effects to the direct photon cross section in nucleus-nucleus collisions was small: less than -25% from the quenching of fragmentation photons, less than $+25\%$ from jet conversion and less than $+10\%$ from medium-induced γ bremsstrahlung. While experimental measurements are not yet precise enough to disentangle such modest effects, they have already put severe constraints on theoretical models that suggest a dominant role of jet-plasma interactions in the $p_T \geq 2$ GeV part of phase space. In particular, PHENIX data is compatible with strong coherent suppression of the bremsstrahlung γ, which is the main theoretical result of this paper.

In conclusion, we suggest that only a systematic study of direct photons in heavy ion reactions for various system sizes and center of mass energies will help uncover their full potential both as a baseline for jet tomography and as an independent probe of nuclear effects. In this exploration, precision d+A data is critical, since our theoretical results support the possibility that, in both proton-nucleus and nucleus-nucleus collisions, cold nuclear matter effects play a dominant role in altering the cross section for direct photon production.

Acknowledgments: We thank T. Goldman and T. Sakaguchi for useful discussions. This research is supported by the US Department of Energy, Office of Science, under Contract No. DE-AC52-06NA25396 and in part by the LDRD program at LANL, the NNSF of China and the MOE of China under Project No. IRT0624.

[1] S. S. Adler *et al.* [PHENIX Collaboration], Phys. Rev. Lett. **94**, 232301 (2005) [arXiv:nucl-ex/0503003].

[2] T. Isobe [PHENIX Collaboration], J. Phys. G **34**, S1015 (2007).

[3] M. Gyulassy, I. Vitev, X. N. Wang and B. W. Zhang, arXiv:nucl-th/0302077.

[4] I. Vitev, Phys. Lett. B **639**, 38 (2006).

[5] A. Adare *et al.* [PHENIX Collaboration], arXiv:0801.4555 [nucl-ex]; K. Reygers, arXiv:0804.4562 [nucl-ex].

[6] D. K. Srivastava, arXiv:0805.3401 [nucl-th].

[7] B. G. Zakharov, JETP Lett. **80**, 1 (2004) [Pisma Zh. Eksp. Teor. Fiz. **80**, 3 (2004)].

[8] S. Turbide, C. Gale, S. Jeon and G. D. Moore, Phys. Rev. C **72**, 014906 (2005).

[9] P. Arnold, G. D. Moore and L. G. Yaffe, JHEP **0112**, 009 (2001); JHEP **0111**, 057 (2001).

[10] M. Gyulassy, P. Levai and I. Vitev, Nucl. Phys. B **594**, 371 (2001).

[11] X. N. Wang and X. F. Guo, Nucl. Phys. A **696**, 788 (2001); B. W. Zhang and X. N. Wang, Nucl. Phys. A **720**, 429 (2003).

[12] R. J. Fries, B. Müller and D. K. Srivastava, Phys. Rev. Lett. **90**, 132301 (2003).

[13] S. Turbide, C. Gale and R. J. Fries, Phys. Rev. Lett. **96**, 032303 (2006).

[14] T. Sakaguchi, arXiv:0805.4644 [nucl-ex].

[15] V. S. Pantuev [PHENIX collaboration], J. Phys. G **34** S805 (2007).

[16] S. Turbide, C. Gale, E. Frodermann and U. Heinz, Phys. Rev. C **77**, 024909 (2008).

[17] F. Arleo, JHEP **0707**, 032 (2007).

[18] J. W. Qiu and I. Vitev, Phys. Lett. B **570**, 161 (2003) [arXiv:nucl-th/0306039].

[19] A. Accardi, arXiv:hep-ph/0212148.

[20] I. Vitev, Phys. Lett. B **562**, 36 (2003).

[21] J. W. Qiu and I. Vitev, Phys. Lett. B **632**, 507 (2006).

[22] K. J. Eskola, V. J. Kolhinen and C. A. Salgado, Eur. Phys. J. C **9** (1999) 61.

[23] I. Vitev, Phys. Rev. C **75**, 064906 (2007).

[24] D. Peressounko [PHENIX Collaboration], Nucl. Phys. A **783**, 577 (2007).

[25] A. Adare *et al.*, arXiv:0801.1665 [nucl-ex].

[26] J. F. Gunion and G. Bertsch, Phys. Rev. D **25**, 746 (1982).

[27] B. W. Zhang and E. K. Wang, Chin. Phys. Lett. **20** (2003) 639.

[28] A. Adil and I. Vitev, Phys. Lett. B **649**, 139 (2007).

[29] A. Majumder, R. J. Fries and B. Muller, arXiv:0711.2475 [nucl-th].

[30] I. Vitev and M. Gyulassy, Phys. Rev. Lett. **89**, 252301 (2002).

[31] Y. Van Haarlem, A. Jgoun and P. Di Nezza, [arXiv:0704.3712 [hep-ex]].

[32] M. Gyulassy, P. Levai and I. Vitev, Phys. Lett. B **538**, 282 (2002).

[33] J. F. Owens, Rev. Mod. Phys. **59**, 465 (1987).

[34] S. S. Adler *et al.* [PHENIX Collaboration], Phys. Rev. Lett. **98**, 012002 (2007).